Spin state transformations of a 3d ion in the pyramidal environment and under lattice distortions

2007 J. Phys.: Condens. Matter 19 156216

(http://iopscience.iop.org/0953-8984/19/15/156216)

IOP PUBLISHING JOURNAL OF PHYSICS: CONDENSED MATTER

J. Phys.: Condens. Matter **19** (2007) 156216 (15pp) doi:10.1088/0953-8984/19/15/156216

Spin state transformations of a 3d ion in the pyramidal environment and under lattice distortions

E S Zhitlukhina[1], K V Lamonova[1], S M Orel[1], P Lemmens[2] and Yu G Pashkevich[1]

[1] A A Galkin Donetsk Phystech NASU, 83114 Donetsk, Ukraine
[2] Institute for Physics of Condensed Matter, D-38106 Braunschweig, Germany

E-mail: y.pashkevich@fkf.mpg.de

Received 14 November 2006, in final form 6 February 2007
Published 26 March 2007
Online at stacks.iop.org/JPhysCM/19/156216

Abstract

Spin state (SS) transitions in metal-containing pyramidal complexes that originate from crystallographic distortions are the research subject of this work. The transition elements are considered to be in the $3d^6$ configuration (Fe^{2+}, Co^{3+}), and they display three different SSs: low-spin (LS, $S = 0$), intermediate-spin (IS, $S = 1$) and high-spin (HS, $S = 2$) states. They have been studied in the frame of the crystal field approximation via the effective nuclear charge Z_{eff} and under oxygen cage distortions. The features of the SS stability have been calculated with/without accounting for spin–orbit coupling. Some critical points at which an accidental degeneracy of the SSs exist have been revealed. Near the critical points, negligible distortions can crucially change the SS. It is demonstrated that the ground SS of the pyramidal MeO_5 complex is very sensitive to the symmetry and magnitude of its distortions. SS diagrams in the parameter space 'effective charge'–'distortion magnitude' have been established. It is revealed that the IS state exists as a ground state for all considered distortions with a corresponding choice of Z_{eff}. Jahn–Teller distortions stabilize the IS state in a wide range of Z_{eff}. The orbital-like reorientation of the electron density distribution was observed for the IS state at some threshold magnitude of Jahn–Teller distortions.

(Some figures in this article are in colour only in the electronic version)

1. Introduction

The study of electronic spin states of 3d metals and spin state transitions are among the most fundamental problems of modern science. It is connected with the contemporary understanding of the role of the electronic spin states as the parameter that governs the physical properties and chemistry of compounds that contain 3d metals. For example, knowledge of the spin state of iron and its possible transformation under compression is important for the interpretation

of seismic observations, geochemical modelling, and geodynamic simulation of the earth's deep interior [1]. The investigation of iron porphyry spin states has an underlying importance in the haemoprotein function with enormous implication for biology, including its role for haem-based receptors, electron transport, oxygen transport, and catalysis [2]. The investigation of structural, calorimetric, magnetic, transport and thermal conductivity data of the cobalt-containing compounds with different oxidation states like $La_{1-\delta}A_{\delta}CoO_3$ (A = Ca, Sr, Ba) allows one to draw conclusions about the effects of strong correlation between all subsystems of such compounds [3–5].

The interest in studying spin transitions has recently been renewed, associated with intense investigations of perovskite-like cobalt-containing compounds such as the rare earth cobaltite $RCoO_3$ [6] (R: rare earth element) or layered cobaltites like $RBaCo_2O_{5+\delta}$ [7], $Sr_{n+1}CO_nO_{2n+1}Cl_n$ [8], or $Ca_3Co_2O_6$ [9]. These compounds are identified as strongly correlated electron systems and they have a set of attractive physical properties. To interpret and to explain these without a consideration and comprehension of the behaviour of their electron subsystem is impossible. A characteristic feature of these compounds is the cobalt ion in the trivalent (3+) state in a $3d^6$ electron configuration, as their electronic spectrum contains energy levels, which correspond to three different spin states, namely, the low-spin (LS) state, the intermediate-spin (IS) state, and the high-spin (HS) state [10, 11]. Transitions between these spin states can be induced by changing the temperature [6, 12] or pressure [13], by applying a magnetic field [14] or by chemical means [15, 16]. The realization of the concrete spin state of a metal ion depends on the ratio between the intra-atomic interactions and the interaction with the surrounding crystal field [3, 4, 17]. One more interesting feature is the proximity of energy of these interactions. The latter one provides the possibility of the stabilization of the intermediate-spin state [3]. Thus, there exists one more degree of freedom, related to an alternation or change of the spin state, which has an effect upon all physical properties of these compounds. Indeed, the unusual temperature dependence of magnetic susceptibility in $LaCoO_3$ as well as the combined semiconductor-to-metal transition and spin state crossover has been discussed within this context. To describe the temperature-induced increase of the susceptibility a varying occupation of levels, which correspond to $S = 0$, $S = 1$ and, finally, $S = 2$ spin states, has been assumed [18–20]. On the other hand, this explanation does agree with the heat capacity data [21]. In contrast, the experimental data were reproduced by a molecular-field model, which proposes that the spin state transition is double-step and that the excited state is a high-spin state [22]. Moreover, the anomalous growth of the resistance and corresponding metal–insulator transition in the layered cobaltites, like $RBaCo_2O_{5.5}$, has convincingly been interpreted assuming a change of spin state [7, 12, 14, 16]. It is interesting to note that both in $LaCoO_3$ and in $RBaCo_2O_{5+\delta}$ the spin state transitions are accompanied by temperature anomalies of the crystal structure parameters [20, 23, 24]. Most remarkable is the behaviour of the crystallographic structure of $RBaCo_2O_{5.5}$ [25–27]. Its elementary cell contains two nonequivalent Co ions: one of them has a five-fold and the other a six-fold coordination. With respect to the total low rhombic symmetry of the crystal, the pyramidal and octahedral complexes are distorted and respond in different ways to changes of temperature. This latter circumstance together with the electronic configuration of the metal ion defines the nontrivial features of its electronic spectrum. One of the interesting questions which have recently been actively discussed in the literature is the question of the origin and stability of the intermediate spin state in such compounds [28].

Potze and co-authors [17] undertook a theoretical study of the intermediate spin state problem as a ground state for a $d^5(d^6)$ system. In terms of ligand fields they proved that the intermediate-spin state is stabilized by the relative stability of the ligand hole state it hybridizes with. Comparing Co 2p x-ray absorption spectra of $SrCoO_3$ with calculations is

compatible with a distortion of the octahedral coordination of the Co ion in the intermediate-spin state. Calculations of the $LaCoO_3$ electronic spectrum using the LDA + U (local density approximation + correlation energy) confirmed that the system is in a nonmagnetic insulating state with spin $S = 0$ at liquid helium temperatures [11]. Note that the Co ion is in an octahedral surrounding of oxygen ions like in $SrCoO_3$. However, it was found that two excited electronic levels, which correspond to $S = 1$ and 2 states, exist and are in proximity to the ground state. With increasing temperatures, these levels are populated. The authors predicate that the band structure of $LaCoO_3$ has some features, namely that e_g-levels of the Co ion form rather wide bands, originating from the hybridization between Co ion d orbitals and surrounding oxygen p orbitals.

Soft-x-ray absorption spectroscopy of the layered cobaltite Sr_2CoO_3Cl revealed that Co^{3+} ions in CoO_5 pyramidal coordination are shifted along the z-axis to the apex oxygen ion and are in the high-spin state [8]. Nevertheless, the calculation of the real crystal structure of this compound with the help of the LDA+U method showed that the IS state can be stabilized if the basal plane corrugation degree $D \leqslant 0.15$ Å (the parameter D represents the average distance between the Co ion and the O_4 basal 'square').

The subjects of this work are spin state transitions in metal-containing pyramidal complexes that originate from crystallographic distortions. As metal ions, we consider transition metal elements with $3d^6$ electronic configuration (for example, Fe^{2+}, Co^{3+}). Distortions, which are most frequently observed in the aforementioned metal oxides, are investigated. These are breathing-like distortions, displacements of the 3d ion along the z-axis, Jahn–Teller-like displacements of the MeO_4 basic pyramidal planes, and corrugation-like MeO_4 plane displacements.

The evolution of the spin state of such metal ions as a function of the 3d-ion effective nuclear charge Z_{eff} and distortions of the oxygen cage is investigated in the frame of the modified crystal field (CF) approximation. In order to describe correctly the effect of spin–orbit interaction and crystal field on the $3d^6$ ion electronic subsystem we used many-particle wavefunctions. Initially, we realize a rough calculation of the metal ion terms without accounting for spin–orbit interaction, and then more accurate calculations are performed including spin–orbit interaction. As a result, spin state diagrams in the parameter space 'metal ion effective charge value'–'distortion magnitude' are calculated. These diagrams demonstrate how changes of the ground spin state depend on the degree of covalency of the Me–O bonds (in this case Z_{eff} is a criterion for the degree of covalency [28, 30]) or on the magnitude of the distortions. The calculations allow conclusions on the sensitivity of the spin ground state of a pyramidal Me–O complex with respect to symmetry and magnitude of the oxygen cage distortions and to the covalency of a Me–O bond. Moreover, they allow us to analyse which distortions stabilize the spin states and to predict the degree to which ion spin states are subject to distortions.

2. Modified crystal field approach

In the pyramidal complex MeO_5 with a metal ion in $3d^6$-electron configuration, the oxygen ions are located in the pyramidal vertices and the metal ion is located in the centre of the basal plane. According to the CF theory main statements, we consider the internal structure of the central ion exactly, while the ligands are considered as structureless, fixed-point charges.

The full many-electron Hamiltonian in the crystal field can represented as follows:

$$H = H_0 + V, \tag{1}$$

where H_0 involves the kinetic energy operators of the electrons and the central atom nuclear;

$V = V_{ee} + V_{SO} + V_{CF}$ is the operator sum of the electron–electron interaction of the d-shell electrons, the spin–orbit ones as well as its interaction with a ligand crystal field, accordingly.

We should recall that ions with the $3d^6$ electron configuration have 16 terms with different multiplicity, which corresponds to 210 states [29–31]. The basic term is ^5D, i.e. five-fold degenerated over the orbital momentum. The analysis of the metal ion spin state using a Hamiltonian in the form of (1) is a rather sophisticated task, as accounting for spin–orbit interaction and arbitrary distortions results in an interaction of all electron terms of the ion. The latter circumstance does not allow one to divide the V perturbation matrix into independent blocks and to simplify the calculations. Moreover, the quantum numbers S^2 and S_z are not good in this general case. This means that energy levels are not ascribed to integer spin values. Therefore, for a simplification of the metal ion spin state analysis it will be appropriate to solve the problem stepwise.

(i) First, a perturbation operator will be considered that does not involve the spin–orbit term, because for the 3d shell the following hierarchy holds: $V_{SO} \ll V_{CF} + V_{ee}$. Thus, the perturbation operator is written as

$$V' = \sum_{i>j}^{6} \frac{e^2}{r_{ij}} + \sum_{k=1}^{N} \sum_{i=1}^{6} \frac{eq_k}{|\vec{r}_i - \vec{R}_k|}. \tag{2}$$

Here, the first term is the electron–electron interaction among d-shell electrons and the second one is the interaction of d electrons with the surrounding crystal field. N is the number of oxygen ions, and $\vec{R}_k$ is the radius vector of the ion with the q_k charge. Now, the quantum numbers S^2 and S_z are fixed and each energy term is determined by the integer value of a spin and an orbital moment.

For the calculation of the eigenvalues of the V' operator we should choose the full orthonormalized system of the many-electron functions. In zero approximation we choose the basic functions of the atomic Hamiltonian $\Psi(\gamma SLM_S M_L)$, which correspond to the $3d^6$ configuration. The functions $\Psi(\gamma SLM_S M_L)$ are the term wavefunctions, which are linear combinations of the *many-electron determinant functions* $\Phi(1, 2, \ldots, 6)$ (the numbers correspond to the one-electron wavefunctions $\psi_i(nlm_l m_s)$ for each of the 3d valence electrons) [29–31]. As one-electron wavefunctions, we take into account hydrogen-like wavefunctions with an effective parameter $a = Z_{eff}/na_0$ (with n the main quantum number and a_0 the Bohr radius).

It is well known, within the frame of the crystal field approximation, that the interaction of the metal ion with the surrounding ligand leads to a splitting of the central ion terms ^{2S+1}L to the crystal ones $^{2S+1}\Gamma$, as well as to a mixing of the terms ($^{2S+1}L\Gamma - {}^{2S+1}L'\Gamma$) of the same symmetry and multiplicity. As a result, the perturbation matrix $V' = V_{CF} + V_{ee}$ divides into three independent blocks with the dimensionalities 5×5, 45×45 and 50×50. The first block conforms to the ^5D term with the spin $S = 2$ and the two others to terms with $S = 1$ and $S = 0$, accordingly. The perturbation matrix elements assume the form

$$V'_{\mu\nu} = \left\langle \Psi_\mu \left(\gamma SLM_S M_L\right) \middle| V' \middle| \Psi_\nu \left(\gamma' SL' M_S M'_L\right) \right\rangle. \tag{3}$$

Here indices μ and ν run through values that are the block dimensionalities.

(ii) The next step of our analysis consists of a more complicated problem—the calculation of the $V = V_{ee} + V_{CF} + V_{SO}$ perturbation matrix. The last component is the spin–orbit interaction; it has relativistic character and, in turn, lifts the degeneracy of crystal levels (so-called fine-structure splitting). The spin–orbit coupling operator can be written in the traditional form:

$$\hat{V}_{SO} = \sum_{i=1}^{6} \xi(r_i)(\hat{l}_i, \hat{s}_i). \tag{4}$$

Here $\xi(r_i)$ is an one-electron constant of a spin–orbit interaction and

$$\xi(r_i) = -\frac{e\hbar^2}{2m^2c^2}\frac{1}{r_i}\frac{\partial U(r_i)}{\partial r_i}; \tag{5}$$

$U(r_i)$ is a field potential in which an electron moves. One can neglect the ligand-field contribution to the field potential $U(r_i)$ because it is smaller than the nuclear-field one. The potential is $U \sim Z$ (here Z is the nuclear charge) when an electron moves in a nuclear field (without taking into account core electrons); then the one-electron constant is $\xi \sim Z^4$. Accounting for the core electrons results in the substitution for $Z \to Z_{\text{eff}}$ in the hydrogen-like functions and the potential is $U \sim Z_{\text{eff}}$. In this case the spin–orbit coupling constant is $\xi \sim Z_{\text{eff}}^4$. These two limiting cases correspond to calculations based on Bohr-like wavefunctions and Slater ones, respectively. However, all of them are not consistent with the available spin–orbit coupling constants λ, which can be extracted from experimental spectral data in the case of Russell–Saunders coupling [32].

$$E_{\text{SO}} = \lambda\hat{S}\hat{L}. \tag{6}$$

Similarly to the monograph [32], we examined different forms of electrostatic potentials and found that the next form of the one-electron spin–orbit coupling constant ξ mainly agrees with a many-electron spin–orbit coupling constant λ [32] (from equation (6)):

$$\xi_{nl} = \frac{\alpha^2}{2}\frac{Z^3 Z_{\text{eff}}}{n^3 l(l+1)(l+1/2)} \quad \text{(at. un.)}, \tag{7}$$

where $\alpha = e^2/\hbar c$ is the fine structure constant. Such a kind of constant corresponds to the matrix elements of operator (5) with the potential $U \sim Z_{\text{eff}}$, which is calculated based on hydrogen-like wavefunctions.

In this case, the perturbation matrix does not divide into blocks of smaller dimensionality, and the matrix elements are

$$V_{\alpha\beta} = \left\langle \Psi_\alpha\left(\gamma S L M_{\text{S}} M_{\text{L}}\right)|V|\,\Psi_\beta\left(\gamma' S' L' M'_{\text{S}} M'_{\text{L}}\right)\right\rangle. \tag{8}$$

Note that the matrix elements (3) and (8) of the perturbation potentials V' and V as well as the eigenvalues of the corresponding secular equation systems depend on the magnitude of Z_{eff}, the ligand charges q_k and the coordinate set of ligands $\vec{r}_k$. Hence, except for the lengths and angles, which characterize the Me–O bonds, as well as the ligand charges, there is one more effective parameter, Z_{eff}, which allows one to take into account the influence of the ligand surrounding on the metal ion state [30]. The spin–orbit bond constant is also a function of the effective charge. This fact allows a parameterization and to account for supplement screening due to the surrounding ligands. We made some rough estimations of the effective nuclear charge changing due to non-local electron density distributions of surrounding ligands.

The screening effect caused by oxygen electrons can be estimated as follows:

$$\Delta E = \langle \Psi_{\text{Me}}|\frac{\int_{V(r_{\text{Me}})}\Psi^*_{\text{lig}}\Psi_{\text{lig}}\,\mathrm{d}V}{r_{\text{Me}}}|\Psi_{\text{Me}}\rangle; \tag{9}$$

here $\Psi_{\text{Me}} = \{\mathrm{d}_{xy}, \mathrm{d}_{xz}, \mathrm{d}_{yz}, \mathrm{d}_{x^2-y^2}, \mathrm{d}_{z^2}\}$, and $\Psi_{\text{lig}} = \{\mathrm{s}, \mathrm{p}_x, \mathrm{p}_y, \mathrm{p}_z\}$; the inner integration has been carried out over a sphere which is centred at the metal site with variable radius r_{Me}. It is clear that ΔE is a function of the type and number of ligands.

The supplement energy contribution, connected with the surrounding crystal oxygen field, makes about 10% of energy of the metal electrons in the field of point charges, for the oxygen pyramidal environment. It allows for changing Z_{eff} in the above-mentioned limits. It is necessary to note that the effective charge values Z_{eff} for free metal ions in the $3\mathrm{d}^6$ electron

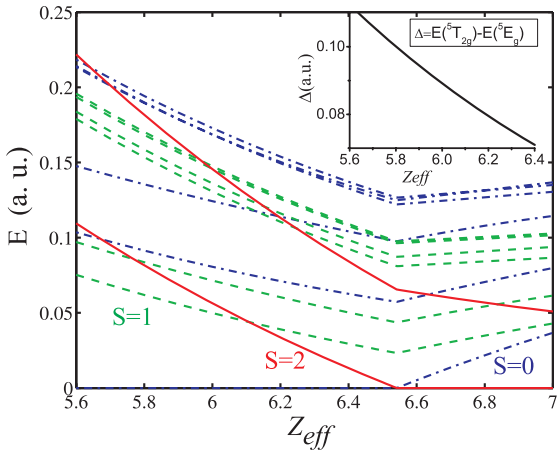

Figure 1. The dependence of some lowest energy levels with different spin states for a $3d^6$ metal ion, which is placed in an octahedral environment, on the effective nuclear charge. Inset: the dependence of crystal field splitting Δ on Z_{eff}.

configuration vary between 6.25 and 7.25 for Fe^{2+} and Co^{3+}, respectively. (The effective charge magnitudes for the free ions are estimated according to Slater's calculations [33].)

To demonstrate the physical meaning of Z_{eff}, a Tanabe–Sugano-like diagram for a $3d^6$ metal ion in an octahedral environment has been calculated (figure 1). We used a regular octahedron with the Me–O distance fixed at 1.95 Å and the ligand's charge equal to -2. Obviously, there is a similarity of energy level dependence on Z_{eff} and the traditional crystal field splitting parameter Δ. As usual, we define this parameter as a splitting of ^5D term into T_{2g} and E_g levels. This splitting decreases when the effective nuclear charge magnitude tends to the free metal ion one, as is shown in the inset of figure 1.

In conclusion, the effective charge and the ligand charges both result in a change of the crystal field. However, the change of Z_{eff} has a more substantial influence on the crystal field value than a change of the ligand charge q_k. Below, we shall consider the ligand charge constant to be equal to -2 (oxygen ions) and vary the effective charge and the ligand coordinates.

3. Results and discussion

3.1. Electronic spectrum of the five-fold coordinated $3d^6$ ions

In this section, we present the calculation results of the lowest electron levels of a metal ion, located in the basic plane of a regular pyramidal complex with Me–O bonds equal to 1.95 Å.

Let us consider the case when the spin–orbit coupling is ignored. Further we will analyse just three lowest energy levels, which correspond to the different spin states (namely, LS, IS and HS). The curves in figure 2(a) demonstrate the dependence of the lowest terms on Z_{eff}, related to LS (black; blue online), IS (light grey; green online) and HS (dark grey; red online) states. Moreover, in figure 2(b) the dependence of the metal spin state $\langle S^2 \rangle$ on Z_{eff} (see grey (red) line) is given. It is obvious that the metal electron subsystem undergoes an HS $\rightarrow$ IS $\rightarrow$ LS transition between the spin states of the metal ion with decreasing effective charge.

These conversions have a stick–slip character and the points $Z_{\text{eff}} = 6.38$ and 5.56 are randomly degenerate points that possess interesting features. At these points any negligible change of the crystal field can lead to spin state fluctuations. These changes can be initiated by different distortions of the complex structure. A symmetry analysis of the electron and

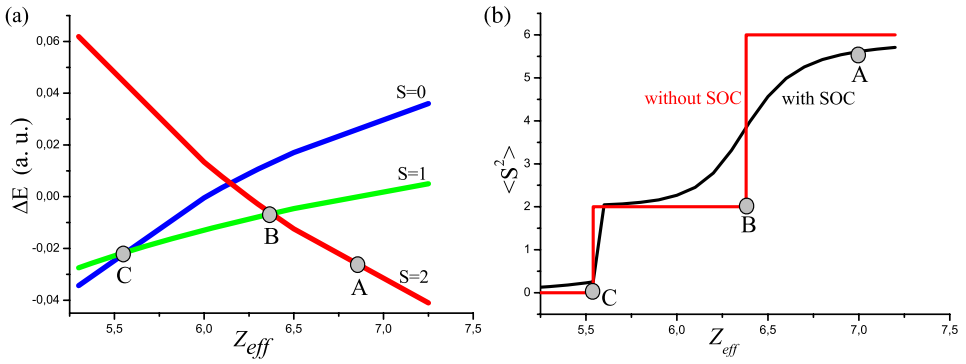

Figure 2. The $3d^6$ metal ion is in the undistorted pyramidal environment of the oxygen ions. Me–O distances are 1.95 Å. (a) The energy dependences of the metal ion electron levels ΔE, which correspond to the three different spin states, on the effective charge value Z_{eff} without accounting for spin–orbit coupling. (b) The dependence of the basic spin state $\langle S^2 \rangle$ on the effective charge value.

vibration levels for the C_{4v} point group reveals that the basic electron levels, which correspond to the high-spin state, are transformed via the E irreducible representation, whereas the $S = 1$ and 0 levels are transformed via the B_1 and A_1 irreducible representations, accordingly. Hence, the random degeneration points are two-fold (point C) or three-fold (point B) degenerated. According to the Jahn–Teller theorem, these points and the E levels are unstable with respect to distortions of various kinds. For example, if the system is at point A, fully symmetric A_1-type vibrations lead to a redistribution of the electron terms leading to an orbital singlet state as the lowest energy state. The A_2-, B_1- and B_2-type vibrations lead to a level splitting. Any vibrations, corresponding to this point group, lift the three-fold degeneration on point B. Finally, B_1-type vibrations lift the two-fold degeneracy at point C only.

However, such drastic changes of the spin state as a function of Z_{eff} are a result of neglecting the spin–orbit interaction (see the red dotted line in figure 2(b)). Otherwise, the dependence $\langle S^2 \rangle$ via Z_{eff} is more complicated: in particular, the LS $\rightarrow$ IS and IS $\rightarrow$ HS conversions become vague (see the black line in figure 2(b)). We denote these as transition vicinities instead of transition points. The LS $\rightarrow$ IS conversion vicinity amounts to 2.5% with respect to $Z_{\text{eff}} = 5.56$, while IS $\rightarrow$ HS is equal to 15% with respect to $Z_{\text{eff}} = 6.38$.

The rather large existence range of the IS ground state is one more distinction of a $3d^6$ configuration from other configurations. Apparently, it is connected with the structure of the spectrum of the $3d^6$ configuration and with peculiarities of the symmetry of the MeO_5 complex. For example, Mn^{3+} and Cr^{2+} ions with a $3d^4$-electron configuration, placed within the same pyramid, do not have such a pronounced feature [27]. We have investigated the spin ground state stability of the 3d ion, and in particular, the IS ground state with respect to the symmetry and magnitude of the ligand distortions. Neglecting spin–orbit interactions we calculated the 3d-ion energy levels, depending on the ligand displacements, for fixed values of Z_{eff}. The choice of the effective charge values are defined by a proximity to the degeneration points. Taking spin–orbit coupling into account we calculated the phase diagrams of the metal ion spin state in the plane (Z_{eff}, Q_i), where Q_i are the normal coordinates corresponding to the respective point group of the symmetry.

3.2. Spin state transformations under MeO_5 complex distortions

We have probed two kinds of complex distortion. These are (I) displacements which preserve the initial MeO_5 complex symmetry, and (II) displacements which lead to a symmetry

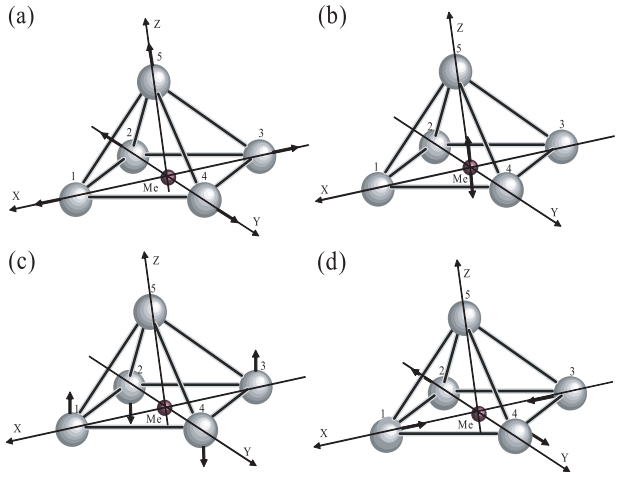

Figure 3. Ion displacement types: (a) the breathing-like distortions; (b) the displacement of the 3d ion along the z-axis; (c) the corrugation-like MeO_4 plane displacements; (d) Jahn–Teller-like displacements of the MeO_4 basic pyramidal plane.

reduction. Breathing-like displacements (figure 3(a)) as well as the displacement of the 3d-ion along the z-axis (figure 3(b)) refer to the first type of distortion and transform via the A_1 irreducible representation of the C_{4v} point group. The corrugation-like MeO_4 plane displacements (figure 3(c)) and Jahn–Teller-like displacements of the MeO_4 basic pyramidal plane (figure 3(d)) concern the second type of distortion and transform via the B_1 irreducible representation of the same point group.

3.2.1. Spin state alteration under breathing-like distortions. Let us consider how the breathing-like distortions affect the behaviour and relative arrangement of the 3d-ion energy levels. First, we should note that such kind of distortions model the phenomenon of thermal lattice expansion/compression due to finite temperatures as well as hydrostatic pressure (figure 3(a)). Figure 4(a) demonstrates the dependence of the lowest energy levels, corresponding to the different spin states, of a homogeneous expansion, which is described by the normal coordinate $Q_1 = (x_1 + y_2 - x_3 - y_4 + z_5)/\sqrt{5}$ (see figure 3(a)). Such distortions are accompanied by a volume change of the pyramid. The calculation shows that the effective charge value determines the expansion/compression value, required for the initialization of spin state transitions. Obviously, the effective charge values as well as the increasing pyramid volume lead to a reduction of the coupling between the metal ion and oxygen surrounding, and hence a decrease of the crystal field. As a result, the Hund's energy Δ_{ex} becomes smaller than the crystal field splitting Δ_{CF} and a corresponding reconstruction of the electron spectrum leads to an HS ground state.

How does spin–orbit coupling affect the spin ground state? The phase diagram of the spin state demonstrates three different areas (see figure 4(b)), which describe the LS (deep blue colour), IS (turquoise colour) and HS (dark red colour) states. In addition, there are two unstable spin state areas. Within the limits of these areas, the spin states are mixed: HS $\leftrightarrow$ IS or IS $\leftrightarrow$ LS. The step-like behaviour in the spin state diagrams is due to the restricted number of fragmentation points. A finer mesh would not be justified as no new physics is expected and the calculation expense is considerable.

As was expected, the HS $\leftrightarrow$ IS unstable area is broader than the IS $\leftrightarrow$ LS one. We marked the spin state of the Fe^{2+} free ion in the phase diagram with $Z_{eff} = 6.25$ and $Q_1 = 0.11$ Å (the

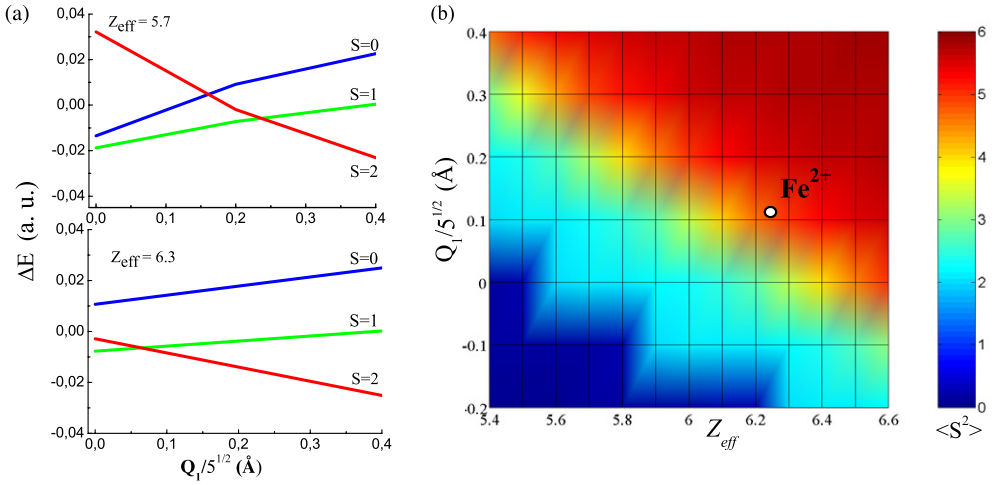

Figure 4. Breathing like-distortions: (a) the lowest energy level behaviours at the two effective charge values without spin–orbit coupling; (b) spin state diagram (Z_{eff}, Q_1). The spin magnitude $\langle S^2 \rangle$ is shown in colour (greyscale) on the right panel.

free ion radii for ions forming the complex, calculated by Shannon [34], are $R_{Fe^{2+}} = 0.74$ Å and $R_{O^{2-}} = 1.32$ Å). One can see that Fe^{2+} is in the HS area in proximity to the HS $\rightarrow$ IS area and a slight decrease of Z_{eff} or Q_1 may lead to a spin state transition. A decrease of the effective charge is equivalent to an enhancement of covalency and leads to a change of spin state. It is easy to see that a rather broad stripe, associated with the IS state, exists. Thus, one can conclude that the IS ground state induced by a certain effective charge can be stabilized by a suitable homogeneous expansion/compression of the pyramidal complex.

3.2.2. Spin state transformations under metal ion shift along the pyramidal Z-axis. In the following, we will consider how other types of distortion affect the energy levels of the metal ions and especially their spin ground state. First, we will discuss a displacement of the central ion with respect to the pyramid basic plane without spin–orbit coupling (see figure 5(a)). This distortion is very important, as in real compounds with metal oxide pyramidal complexes the metal ions are often shifted out of the pyramid plane. It can be described by the normal coordinate $Q_2 = z_{\text{Me}}$ that transforms via the A_1 irreducible representation of the C_{4v} point group (see figure 3(b)). Thus, this distortion is fully symmetric and preserves the degeneracy of the given crystal field symmetry. Such distortions do not modify the volume of the complex; however, they lead to a modification of the covalence of Me–O bonds due a redistribution of the electron density. The crystal field value depends on the direction of the metal ion displacement. While an ion displacement into the pyramid results in an increasing crystal field, the reverse direction leads to a decreasing crystal field. Therefore, we should expect spin transitions like IS $\rightarrow$ HS and IS $\rightarrow$ LS with a displacement into and out of the pyramid. Indeed, a similar behaviour of the basic terms is observed at $Z_{\text{eff}} = 5.7$ (figure 5(a)). Nevertheless, with a more effective charge value (for example, $Z_{\text{eff}} = 6.3$) the electron term layout is more complex. The intermediate spin state remains the ground state in a small range of displacements. A small Me ion displacement in either direction leads to the HS state (points C and D in figure 5(a)). Note that the HS state level transforms via E, i.e. it is two-fold degenerate. The latter is given by crystal field symmetry and is unstable due to the Jahn–Teller theorem.

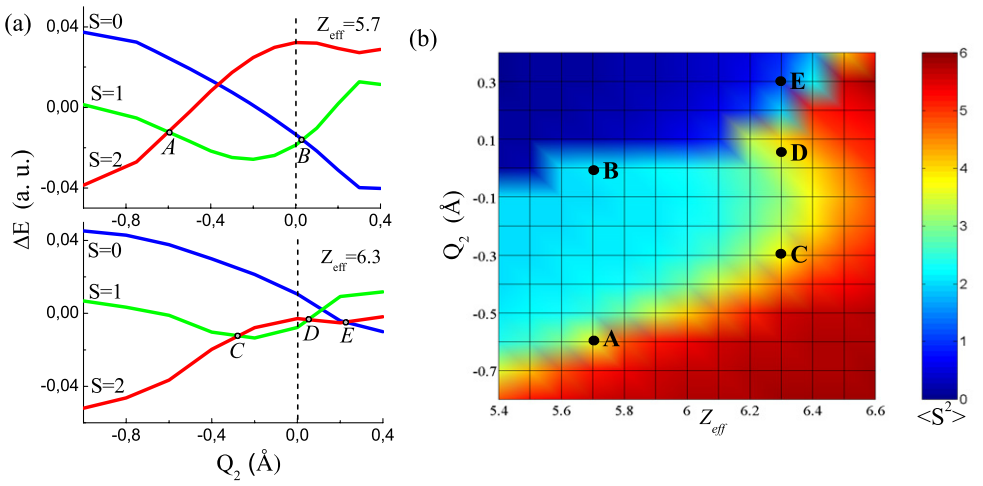

Figure 5. Displacement of the 3d ion along the z-axis: (a) the lowest energy level behaviours at two effective charge values without spin–orbit coupling; (b) spin state diagram (Z_{eff}, Q_2).

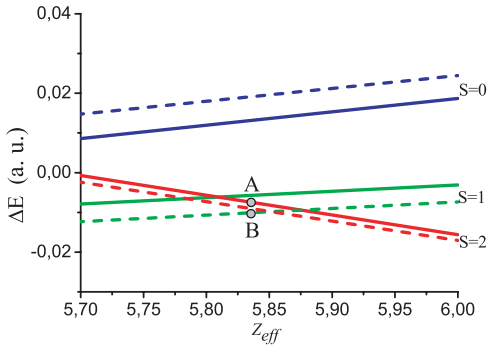

Figure 6. The lowest energy levels for the real compound Sr_2CoO_3Cl with the Co ion in the pyramidal environment. Solid lines correspond to the off-centre position of the Co ion towards the apex oxygen (the displacement is equal to 0.325 Å); dashed lines correspond to the centred position of the Co ion in the basal pyramid plane. Here we used the structural data for Sr_2CoO_3Cl listed in the paper by Loureiro *et al* [8].

The level intersection points (A, B, C, D, E) in figure 5(a) are transitions with different random degeneration. One should expect that such degeneration will be lifted if spin–orbit coupling is taken into account. The energy distance between the levels at these points is comparable with the fine structure splitting. Therefore, the points A, B, C, D, and E in the spin state diagram (figure 5(b)) lie in unstable regions with mixed spin states.

It is interesting to compare the results of our crystal field approach and more sophisticated LDA + U calculations for the real metal oxide Sr_2CoO_3Cl [8]. One can see in figure 6 that if the Co ion has effective nuclear charge within the limits of $5.815 < Z_{\text{eff}} < 5.875$, then its displacement along z-axis to the apex oxygen results in HS $\leftrightarrow$ IS conversion. Indeed, if the Co ion is off-centre at 0.325 Å into the pyramid it is in the HS state (point A in the red solid line), while at the same effective nuclear charge, a Co ion which is placed in the centre of basal pyramidal plane is in the IS state (point B in the green dashed line). Exactly this tendency has been stressed in the paper by Wu [8].

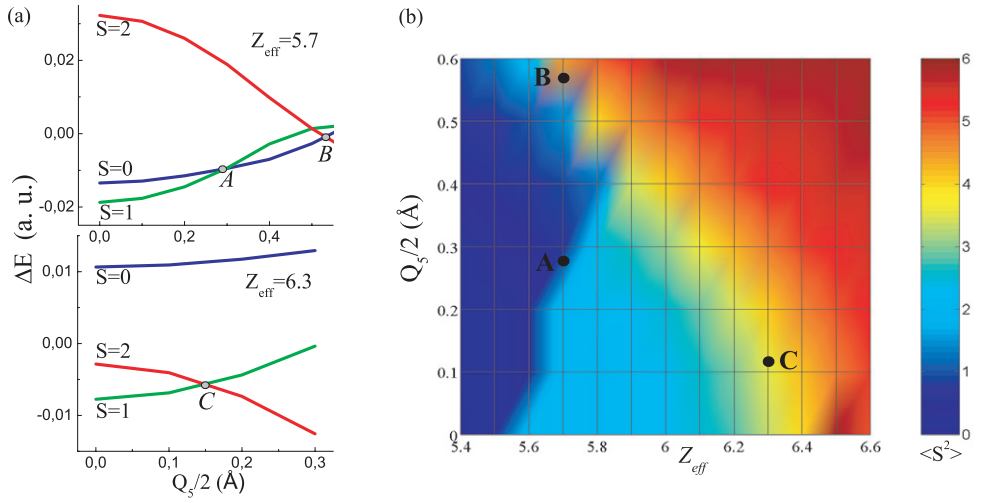

Figure 7. Corrugation-like MeO_4 plane displacements: (a) the lowest energy level behaviours at the two effective charge values without spin–orbit coupling; (b) spin state diagram (Z_{eff}, Q_5).

3.2.3. The influence of corrugation-like MeO_4 plane distortions on the metal ion spin state. One more distortion type—corrugation-like MeO_4 plane displacements (see figure 3(c))—was considered in this study. A basic plane corrugation is a characteristic displacement for perovskite-like cobalt-containing oxides and layered cobaltites [24]. Such displacements are described by the $Q_5 = (z_1 - z_2 + z_3 - z_4)/2$ normal coordinate, which transforms via the B_1 irreducible representation and does not lead to a volume change, but reduces the complex symmetry. As a result, the Me–O bonds in the pyramid basic plane become non-equivalent; the latter leads to an additional low-symmetry splitting of the crystal levels.

Note that the corrugation-like plane displacements lead to a nontrivial transition set IS $\rightarrow$ LS $\rightarrow$ HS at $Z_{\text{eff}} = 5.7$ (points A and B in figure 7(a)). The term alternations at the more effective charge value are traditional: the IS state gives place to the HS state (C is the transition point). In contrast to the above-mentioned full-symmetry distortion, this kind of distortion lifts the crystal symmetry degeneration. As a result, all basic energy levels with different spin states are orbital singlets, and the intersection points like A, B and C are two-fold degenerate (see figure 7(a)). Accounting for spin–orbit coupling can eliminate such degeneracy. Indeed, if one looks at the spin state diagram in figure 7(b) one can conclude that the most probable low-spin state is at point A, whereas a high-spin state is realized at point B. As for point C, it is in a mixed region with an indefinite spin state. It is shown that the phase space of the intermediate-spin state decreases with increasing corrugation.

3.2.4. Intermediate spin state stabilization and electron density redistribution under Jahn–Teller distortions. The final and most important kinds of distortions considered in this paper are Jahn–Teller-like distortions (figure 3(d)). The corresponding displacements are described by $Q_4 = (x_1 - y_2 - x_3 + y_4)/2$, which transforms via the B_1 irreducible representation. They do not change the volume but reduce the C_{4v} pyramid symmetry up to C_{2v} due to the basic plane transformation into a rhomb. It is frequently observed in real materials like layered cobaltites $RBaCo_2O_{5.5}$ and others. Moreover, it is generally accepted that the Co^{3+} ions which are placed in the pyramid sites in layered cobaltites are in the intermediate-spin states for a wide

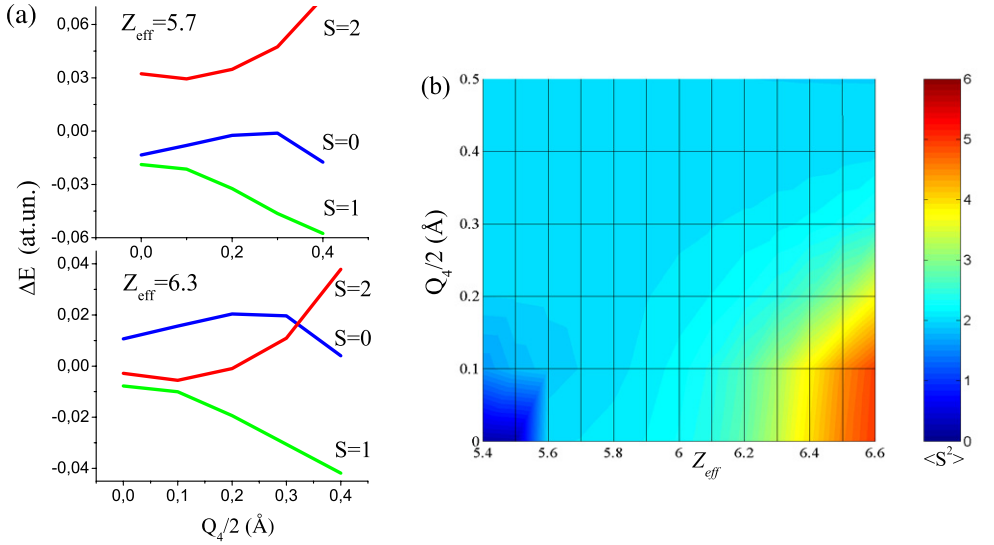

Figure 8. Jahn–Teller-like displacements of MeO_4 basic pyramidal plane: (a) the lowest energy level behaviours at the two effective charge values without spin–orbit coupling; (b) spin state diagram (Z_{eff}, Q_4).

temperature range [12, 26, 35]. In this situation, the effect of temperature on the pyramidal complex can be modelled by Jahn–Teller distortion changes.

The present calculation (see figure 8) agrees with this experimental fact [12, 26, 35]. Obviously, the electron subsystem of the Co ion possesses characteristic features, namely, the IS state is the ground state in a large parameter space of effective charge and Jahn–Teller-like distortions. An increase of the effective charge reduces the energy level which corresponds to the HS state, and as a result leads to a traditional Hund's population of electron levels as for undistorted and slightly distorted pyramids. In contrast, a decrease of Z_{eff} reduces the energy levels with $S = 0$ and at $Z_{\text{eff}} < 5.6$ the LS state becomes the ground state.

There is one more important feature of the electron subsystem behaviour under Jahn–Teller- like distortions. The lowest IS state level undergoes a character break at some critical point $Q_4/2 = 0.1$ Å (figure 8(a)). It originates from the crossing of electron levels with the same spin but with different space symmetry. Otherwise, the electron subsystem tunes to Jahn–Teller lattice distortion (see figure 3(d)) and the more appropriate electron density distribution gains lowest energy. For a one-electron wavefunction (i.e. for a d^1 ion) this change is connected with orbital reorientation. However, in our case we are dealing with a many-electron wavefunction with a complex contribution of different orbital states. Thus, the real electron density distribution has a much more complicated character and just mimics one-electron orbital reorientation (see figure 9). Comparing figures 8(a) and 9 one can conclude that this orbital-like reorientation takes place at some threshold magnitude of the Jahn–Teller distortion.

4. Conclusion

The dependence of the spin ground state of a metal ion with $3d^6$ electron configuration on the oxygen cage distortions has been calculated within a crystal field technique. This

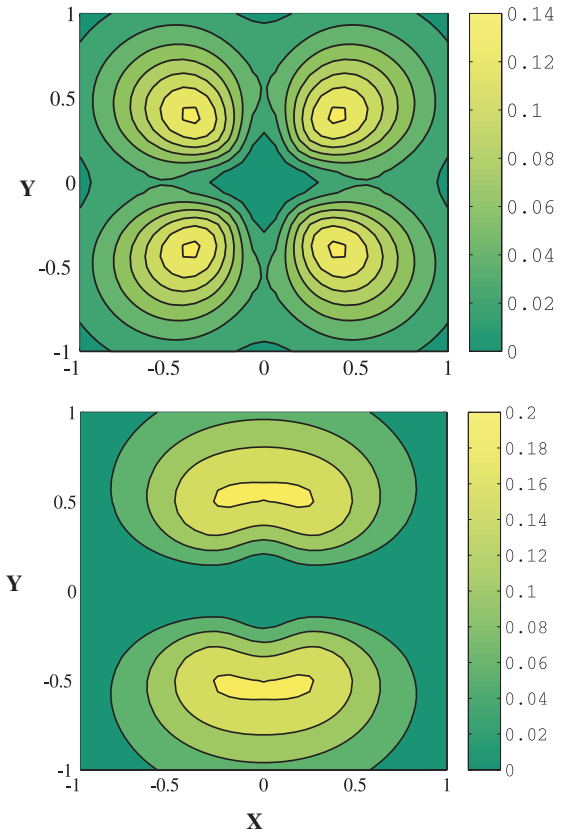

Figure 9. Electronic density redistribution of the d shell in the basic pyramidal plane for $Z_{\text{eff}} = 5.7$: (upper panel) undistorted pyramid; (lower panel) Jahn–Teller-like distorted pyramidal plane, $Q_4/2 = 0.4$ Å. The colour bar represents the electronic density. The metal ion is placed at the centre of basic plane at the (0, 0) point; oxygen ions are placed at ($\pm$1.95 Å; 0) and (0; $\pm$1.95 Å) in the upper panel and at ($\pm$1.55 Å; 0) and (0; $\pm$2.35 Å) in the lower panel.

analysis shows that different kinds of distortion lead to different scenarios of the electron term behaviours. As a result, different spin state diagrams have been obtained. The comparison of the spin state distributions in the diagrams has shown that the spin ground state of the pyramidal Me–O complexes is very sensitive to the symmetry and the magnitude of the oxygen cage distortions.

Some conclusions were made as for the IS state: (a) it is stabilized with a change of the MeO_5 complex volume and a change of the effective charge; (b) an Me ion displacement stabilizes the IS state; however, the enhancement of the effective charge, Z_{eff}, leads to a decreasing of the IS phase space; (c) the IS state region decreases as the corrugation increases; (d) Jahn–Teller distortions stabilize the IS state in a wide range of Z_{eff} (this is consistent with experimental observations in layered cobaltites); (e) the orbital-like reorientation of electron density distribution was observed for the IS state at some threshold magnitude of Jahn–Teller distortions.

Some critical points were revealed as randomly degenerate points versus spin state. The nature of this degeneracy was investigated. It was revealed that fully symmetric distortions, such as breathing-like distortions and a displacement of the 3d ion along the z-axis, do not

lift degeneracy but rearrange only the electron terms. Low-symmetry ion displacements, for example, Jahn–Teller-like displacements and corrugation-like MeO_4 plane displacements, lead to an additional level splitting. Moreover, accounting for spin–orbit interaction mixes the different spin states at the critical points and, as a result, areas with instabilities appear. Near these spin-mixed regions distortions with negligible magnitudes can crucially influence the spin state of the 3d ion.

Acknowledgments

This work was supported in part by grant INTAS 01-0278 and the DFG within the priority program Molecular Magnetism.

References

[1] Gaffney E S and Anderson D L 1973 *J. Geophys. Res.* **78** 7005
Burns R G 1993 *Mineralogical Applications of Crystal Field Theory* (Cambridge: Cambridge University Press)
[2] Scheidt W R and Reed C A 1981 *Chem. Rev.* **81** 543
Kadish K M, Smith K M and Guilard R 2000 *The Porphyrin Hand Book* (San Diego, CA: Academic)
[3] Goodenough J B and Raccah P M 1965 *J. Appl. Phys. Suppl.* **36** 1031
[4] Raccah G P M and Goodenough J B 1967 *Phys. Rev.* B **155** 932
[5] Briceno G, Chang H, Sun X, Schultz P G and Xiang X D 1995 *Science* **270** 273
[6] Asai K, Gehring P, Chou H and Shirane G 1989 *Phys. Rev.* B **40** 10982
Asai K, Yokokura O, Nishimori N, Chou H, Tranquada J M, Shirane G, Higuchi S, Okajima Y and Kohn K 1994 *Phys. Rev.* B **50** 3025
[7] Martin C, Maignan A, Pelloquin V, Nguyen N and Raveau B 1997 *Appl. Phys. Lett.* **71** 1421
Maignan A, Martin C, Pelloquin D, Nguyen N and Raveau B 1999 *J. Solid State Chem.* **142** 247
Wu H 2000 *Phys. Rev.* B **62** 11953(R)
Wu H 2001 *Phys. Rev.* B **64** 092413
[8] Hu Z, Wu H, Haverkort M W, Hsieh H H, Lin H-J, Lorenz T, Baier J, Reichl A, Bonn I, Felser C, Tanaka A, Chen C T and Tjeng L H 2004 *Phys. Rev. Lett.* **92** 207402
Wu H 2002 *Eur. Phys. J.* B **30** 501
Loureiro S M, Felser C, Huang Q and Cava R J 2000 *Chem. Mater.* **12** 3181–5
[9] Maignan A, Michel C, Masset A C, Martin C and Raveau B 2000 *Eur. Phys. J.* B **15** 657
[10] Sugano S, Tanabe Y and Kamimura H 1970 *Multiplets of Transition-Metal Ions in Crystals* (New York: Academic)
[11] Korotin M A, Ezhov S Yu, Solovyev I V, Anisimov V I, Khomskii D I and Sawatzky G A 1996 *Phys. Rev.* B **54** 5309
[12] Morimoto Y, Akimoto T, Takeo M, Mashida A, Nishibori E, Takata M, Sakata M, Ohoyama V and Nakamura A 2000 *Phys. Rev.* B **61** 13325(R)
[13] Asai K, Yokokura O, Suzuki M, Naka T, Matsumoto T, Takaha H, Môri N and Kohn K 1997 *J. Phys. Soc. Japan* **66** 967
Vogt T, Hriljac J A, Hyatt N C and Woodward P 2003 *Phys. Rev.* B **67** 140401(R)
Lengsdorf R, Ait-Tahar M, Saxena S S, Ellerby M, Khomskii D I, Micklitz H, Lorenz T and Abd-Elmeguid M M 2004 *Phys. Rev.* B **69** 140403(R)
Orlovskaya N, Steinmetz D, Yarmolenko S, Pai D, Sankar J and Goodenough J 2005 *Phys. Rev.* B **72** 014122
Zhou J-S, Yan J-Q and Goodenough J B 2005 *Phys. Rev.* B **71** 220103(R)
Fita I, Szymczak R, Puzniak R, Troyanchuk I O, Fink-Finowicki J, Mukovskii Ya M, Varyukhin V N and Szymczak H 2005 *Phys. Rev.* B **71** 214404
[14] Respaud M, Frontera C, García-Muñoz J L, Aranda M Á G, Raquet B, Broto J M, Rakoto H, Goiran M, Llobet A and Rodrígues-Carvajal J 2001 *Phys. Rev.* B **64** 214401
[15] Troyanchuk I O, Kasper N V, Khalyavin D D, Szymczak H, Szymczak R and Baran M 1998 *Phys. Rev.* B **58** 2418
Vanitha P V, Arulraj A, Santhosh P N and Rao C N R 2000 *Chem. Mater.* **12** 1666
[16] Frontera C, Respaud M, García-Muñoz J L, Llobet A, Carillo A E, Caneiro A and Broto J M 2004 *Physica* B **346/347** 246

[17] Potze R H, Sawatzky G A and Abbate M 1995 *Phys. Rev.* B **51** 11501
[18] Maris G, Ren Y, Volotchaev V, Zobel C, Lorenz T and Palstra T T M 2003 *Phys. Rev.* B **67** 224423
[19] Asai K, Yoneda A, Yokokura O, Tranquada J M, Shirane G and Kohn K 1998 *J. Phys. Soc. Japan* **67** 290
[20] Radaelli P G and Cheong S-W 2002 *Phys. Rev.* B **66** 094408
[21] Stolen S, Gronvold F, Brinks H, Atake T and Mori H 1997 *Phys. Rev.* B **55** 14103
Kyômen T, Asaka Y and Itoh M 2003 *Phys. Rev.* B **67** 144424
[22] Kyômen T, Asaka Y and Itoh M 2005 *Phys. Rev.* B **71** 024418
[23] Kwon S K, Park J H and Min B I 2000 *Phys. Rev.* B **62** R14637
[24] Xu S, Morimoto Y, Mori K, Kamiyama T, Saitoh T and Nakamura A 2001 *J. Phys. Soc. Japan* **70** 3296
[25] Frontera C, García-Muñoz J L, Llobet A, Aranda M Á G, Rodrígues-Carvajal J, Respaud M, Broto J M, Raquet B, Rakoto V and Goiran M 2001 *J. Alloys Compounds* **323/324** 468
Frontera C, García-Muñoz J L, Llobet A, Mañosa Ll and Aranda M Á G 2003 *J. Solid State Chem.* **171** 349
[26] Frontera C, García-Muñoz J L, Llobet A and Aranda M Á G 2002 *Phys. Rev.* B **65** 180405(R)
[27] Chernenkov Yu P, Plakhty V P, Fedorov V I, Barilo S N, Shiryaev S V and Bychkov G L 2005 *Phys. Rev.* B **71** 184105
[28] Zhitlukhina H, Lamonova K V, Orel S M and Pashkevich Yu G 2005 *Low Temp. Phys.* **31** 963
[29] Bersuker I B 1996 *Electronic Structure and Properties of Transition Metal Compounds: Introduction to the Theory* (New York: Wiley–Interscience)
[30] Condon E U and Shortely G H 1935 *The Theory of Atomic Spectra* (New York: Cambridge University Press)
[31] Sobel'man I I 1972 *Introduction to the Theory of Atomic Spectra* (New York: Pergamon)
[32] Dunn T M 1961 *Trans. Faraday Soc.* **57** 1441
[33] Slater J 1930 *Phys. Rev.* **36** 57
[34] Shannon R D 1972 *Acta Crystallogr.* A **32** 751
[35] Fauth F, Suard E and Caignaert V 2001 *Phys. Rev.* B **65** 060401(R)